

**Development of Rare-earth-free Phosphors for Eco-energy
Lighting Based LEDs**

Journal:	<i>Journal of Materials Chemistry C</i>
Manuscript ID:	TC-ART-05-2015-001516.R1
Article Type:	Paper
Date Submitted by the Author:	05-Aug-2015
Complete List of Authors:	Boonsin, Rachod; ENSCCF, Chimie Chadeyron, Geneviève; ENSCCF, Chimie Roblin, Jean-Philippe; ENSCCF, Chimie BOYER, Damien; Clermont University, Laboratory of inorganic materials Mahiou, Rachid; LMI Clermont-Ferrand,

ARTICLE

Development of Rare-earth-free Phosphors for Eco-energy Lighting Based LEDs

Cite this: DOI: 10.1039/x0xx00000x

Rachod Boonsin,^a Geneviève Chadeyron,^{*ac} Jean-Philippe Roblin,^{ac} Damien Boyer,^{ac} and Rachid Mahiou^{bc}

Received 00th January 2012,
Accepted 00th January 2012

DOI: 10.1039/x0xx00000x

www.rsc.org/

Several phosphors without rare-earth elements were synthesized by a simple and practical method. Depending on their wavelength emitting range upon UV excitation, i.e. blue, green or red, they were classified in three groups. The phosphors exhibiting the best performances in optical properties were selected to be incorporated in free-standing silicon films and combined with a 365 nm LED. The thermal quenching of phosphors as well as the photometric parameters of the luminescent composite films were investigated. This white emission of the combination between the rare-earth-free phosphors based silicon film and LED shows a CRI > 75 and CCT around 4000K which can fulfil the requirements for indoor domestic lighting source.

Introduction

White light emitting diodes (WLEDs) have reached efficiencies which should allow them to be candidates as light sources for future domestic indoor lighting.¹ The great interest in these WLEDs arises from their unique properties including low power consumption, environmental friendliness, small volume and long lifetime, making these devices very promising candidates to replace presently used incandescent and fluorescent lamps.²⁻⁵ Current commercial WLEDs consist of a 460 nm InGaN blue LED chip combined with Ce-doped yttrium aluminum garnet (YAG: Ce) phosphor, which efficiently convert the blue light arising from the LED into a very broad yellow emission band, producing a white light.

However, this association suffers from some weaknesses such as poor color rendering index (CRI) and low stability of color temperature. Actually, in such a device, the deterioration of the chip or the YAG: Ce phosphor can result in significant color changes. Moreover, the color temperature of the combination is much too cold for indoor domestic lighting (> 4500 K) due to a lack of red contribution. These drawbacks prevent this type of WLEDs from penetrating the general lighting market. In particular, the highly valued indoor domestic lighting requires a CRI better than 90, the color temperature comprises between 3000 and 4000 K with a

luminous efficiency should be greater than or equal to 150 lumen per watts.⁶⁻⁸ Combining deep-ultraviolet (DUV – 200 nm ≤ λ_{em} ≤ 300 nm) or near-ultraviolet (UV – 300 nm ≤ λ_{em} ≤ 400 nm) diode chips with a mixture of red, green and blue phosphors for producing white light appears as a promising alternative with several advantages for a better control of photometric parameters. One of the key points of this combination is an invisible emission of the LED chip contrary to blue chip.⁶ This device can dominate a large panel of applications notably because they give access to the wide range of luminance and the tunable color rendering index (CRI) value. The versatility of the combination “UV LED/phosphors” is due to the possibility to play with the phosphors formulation, using the suitable phosphors with such an excitation, as well as the phosphors ratio. However, at this stage, according to the lighting market players, the aim of this combination in the lighting market should keep its focus on improving the UV LEDs technology, especially for DUV LEDs which still exhibit inadequate performances.⁹⁻¹² In recent years, the remote phosphors, which combine the UV/blue chip and phosphors in appreciable distance, have been investigated.¹³⁻¹⁵ This kind of combination between LEDs and phosphors is of interest because these remote-type phosphor-LEDs overcome some technological limitations including thermal degradation of organic phosphors, light extraction efficiency and light distribution within remote-type designed packaging.

Today, according to the materials currently used, several problems have been identified. For example, the availability of rare earth materials is being affected by rising their prices and limiting the export products imposed by rare earth producing countries.¹⁶ Thus, the development of alternative phosphors such as rare-earth-free phosphors¹⁷⁻²⁰ to preserve natural resources is highly important.

^aUniversité Clermont Auvergne, ENSCCF, Institut de Chimie de Clermont-Ferrand, BP 10448, F-63000 Clermont-Ferrand, France.

^bUniversité Clermont Auvergne, Université Blaise Pascal, Institut de Chimie de Clermont-Ferrand, BP 10448, F-63000 Clermont-Ferrand, France.

^cCNRS, UMR 6296, ICCF, F-63171 Aubière, France.

*E-mail : Geneviève.Chadeyron@univ-bpclermont.fr;
Tel. : +33 (0)4 73 40 71 09; Fax : +33 (0)4 73 40 71 08.

† Electronic supplementary information (ESI) available:
Experimental procedures and additional data of luminescent
compounds. See DOI: 10.1039/b000000x/

Additionally, the upfront cost of LED-based lighting remains too high to fully compete with incumbent technologies. Indeed a comparison of average selling price of different lamp technologies shows that the price of LED lamps is ten times higher than the incandescent bulbs and two times higher than the fluorescent lamps. Moreover, the cost of LED lights is directly dependent on the rare earth fares, in that the phosphors consisting of rare earth elements present about 12% of the cost of a LED lamp. As a consequence, the development of phosphors without rare earth elements represents an important challenge for the expansion of the white LEDs market.

The rare-earth-free phosphors based on luminescent compounds can be considered as an alternative solution thanks to the good low-cost precursors, and several ways to tune-up the colours by playing with their functional groups.

In this work, we report the synthesis of rare-earth-free phosphors, two purely inorganic and one metallo-organic, based on 2, 6-dimethyl-4-pyrone and Schiff based ligand. Their morphological and optical characteristics have been studied. The phosphors exhibiting the best performances in absolute quantum yields (%QE) were assessed in thermal stability at an equivalent temperature of remote phosphors for LED lighting.²¹ In final state, the composite films constituted of silicone and selected phosphors have been prepared to undergo testing using UV / blue LEDs devices in remote phosphor systems for large scale experiment.

Experimental

Materials

All the materials were purchased and used as received. Solvents were distilled prior to use.

Synthesis of phosphor 1

A mixture of (2,6-dimethyl-4H-pyran-4'-ylidene)malononitrile (1mmol), hexylamine (1mmol), in acetonitrile (50 mL) was heated under reflux until completion (TLC monitoring). After cooling down to room temperature, the solutions were concentrated under pressure then filtered and washed several times with ethanol. Purification by crystallization gave the 2-(1-hexyl-2, 6-dimethylpyridin-4H-ylidene)malononitrile (2c) as a white solid: yield (80%). mp 170.2-171.1°C (from acetonitrile). $\nu_{\max}/\text{cm}^{-1}$ 2951, 2926 (CH₂, CH₃), 2186 (C≡N), 2165, 1633 (C=C), 1550, 1496, 1363, 1184, 1064, 839, 540. δ_{H} (400 MHz; CDCl₃) 6.63 (s, 2H), 3.91 (t, $J = 8.4$ Hz, 2H, CH₂), 2.47 (s, 6H, CH₃), 1.75-1.64 (m, 2H, CH₂), 1.47-1.29 (m, 6H, CH₂ chain), 0.92 (t, $J = 7.2$ Hz, 3H, CH₃). δ_{C} (100 MHz; CDCl₃): 155.6, 147.6, 118.8, 113.7, 49.1, 31.0, 29.4, 26.2, 22.3, 20.5, 13.7. MS (ESI) m/z : [M+H]⁺ calcd for C₁₆H₂₂N₃ 256.1814, found 256.1802.

Synthesis of phosphor 2

A mixture of (2,6-dimethyl-4H-pyran-4'-ylidene)malononitrile (1mmol), benzaldehyde (2mmol), piperidine (2mmol) in acetonitrile (50 mL) was heated under reflux until completion (TLC monitoring). After cooling down to room temperature, the precipitate solids was filtered and washed several times with cold methanol. Purification by crystallization gave the 2-(2,6-distyryl-4H-pyran-4'-ylidene)malononitrile (4a) as an orange-

red solid: yield (44%). mp 252.9-253.4°C (from acetonitrile/dichloromethane). $\nu_{\max}/\text{cm}^{-1}$ 2207 (C≡N), 1642 (C=C), 1608, 1541, 1500, 1417, 1330, 1304, 1197, 1180, 972, 943, 831, 756, 697, 481. δ_{H} (400 MHz; CDCl₃) 7.63-7.58 (dd, 3H, Ar, $J = 7.5$, 1.65 Hz), 7.56 (d, $J = 16.1$ Hz, 2H, trans C=C), 7.50-7.43 (m, 6H, Ar), 6.79 (d, $J = 16.1$ Hz, 2H, trans C=C), 6.72 (s, 2H). δ_{C} (100 MHz; CDCl₃): 158.4, 156.1, 138.4, 134.8, 130.8, 129.5, 128.1, 118.8, 115.4, 107.6.

Synthesis of phosphor 3 (5)

Synthesis of MPBH ligand (5a): the product was prepared according to reference.²² Benzhydrazide (1mmol) and 2-acetylpyrazine (1mmol) are added in ethanol. The reaction mixture is refluxed overnight. The reaction mixture is cooled down to room temperature and the solvent is evaporated. The crude solid is recrystallized in ethanol afford 5a as a white crystal: yield (45%). mp 175.8-177.1°C (from ethanol). $\nu_{\max}/\text{cm}^{-1}$ 3380, 3054, 1688, 1599, 1579, 1532, 1516, 1492, 1467, 1427, 1407, 1365, 1324, 1254, 1172, 1155, 1141, 1126, 1075, 1047, 1017, 905, 841, 801, 755, 713, 688, 658, 580, 504, 480, 453, 421. δ_{H} (400 MHz; DMSO-d₆) 11.05 (s, 1H, NH), 9.25 (s, 1H), 8.69-8.60 (d, 2H), 7.88 (s, 2H), 7.64-7.49 (m, 3H), 2.45 (s, 3H, CH₃). δ_{C} (100 MHz; DMSO-d₆) 150.1, 144.2, 142.2, 141.1, 133.0, 131.5, 128.2, 127.8, 127.0, 126.7, 21.4. MS (ESI) m/z : [M+H]⁺ calcd for C₁₃H₁₃N₄O, 241.1089, found 241.1081.

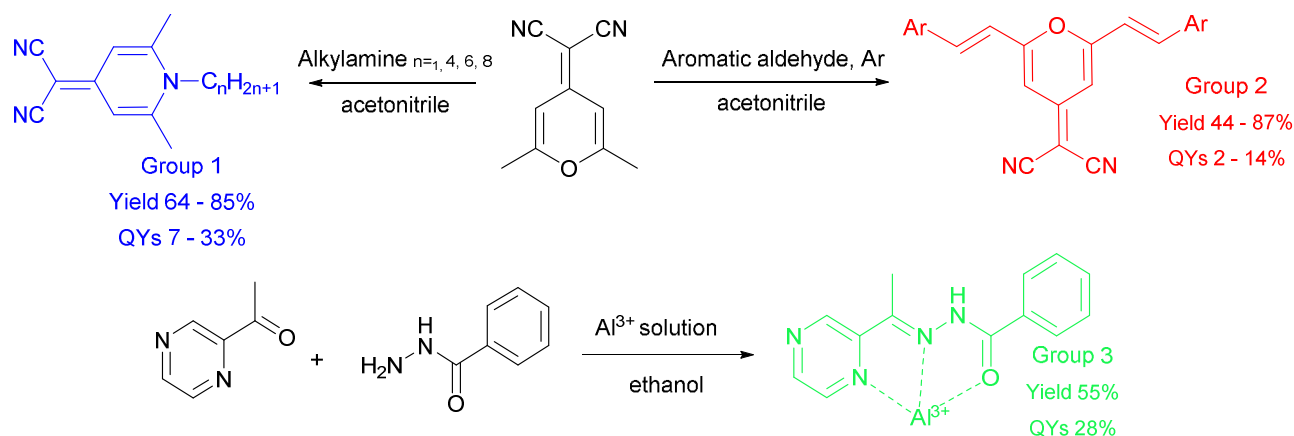
Synthesis of Al-MPBH complex (5b): the product was then synthesized by addition of aluminium nitrate nonahydrate (1mmol) to a solution containing of MPBH (1mmol) in ethanol. The reaction mixture is then refluxed for 2 hrs. The precipitate solid is filtered, washed with ethanol and dried at 50°C in vacuum. The final product 5b affords as a green powder: yield (55%). mp>300°C. $\nu_{\max}/\text{cm}^{-1}$ 3600-2500 (broad), 1639, 1599, 1585, 1508, 1469, 1435, 1388, 1327, 1296, 1203, 1153, 1072, 1045, 725, 694, 660, 574. δ_{H} (400 MHz; DMSO-d₆) 9.70 (s, 1H), 9.44 (s, 1H), 9.14 (s, 1H), 8.71-8.53 (m, 1H), 8.30-8.00 (m, 1H), 7.80-7.46 (m, 2H), 2.62 (s, 3H, CH₃). MS (ESI) m/z : [MPBH+Al+3NO₃+CH₃OH+H₂O]⁺ found for Al-MPBH complex, 503.1963.

Preparation of composite films

A mechanic mixing was applied in order to obtain a well-dispersed mixture composed of the phosphors and the silicone resin. The solution composite was deposited on a Teflon sheets by means of an Erichsen 809MC. The space between the blade knife and the Teflon surface was between 100 – 300 μm and the casting speed was fixed at 25 mm/s. The films were obtained after drying at 50°C for 4 hours and 24 hours at room temperature. The free standing films were then achieved and used for spectroscopic analysis. The film thickness was measured by a CADAR-MI20 micrometer. It should be noted that, however, the composite films are opaque but slightly translucent due to the thickness and the variation of composition of phosphors in the films. The maximum concentration of phosphors in the composite films was fixed at 15%w/w.

Characterization techniques

Thin layer chromatography analysis (TLC) was performed on pre-coated aluminium backed silica plates 60 with fluorescent indicator UV254. Micrographs were recorded using a Cambridge Scan 360



QYs = absolute quantum yield = (number of photons emitted/number of photons absorbed) x absorption

Fig. 1 Synthesis routes for rare-earth-free phosphors.

SEM operating at 20 kV. All specimens were prepared on a surface of an adhesive carbon film. ^1H and ^{13}C NMR spectra were recorded with a Bruker AVANCE spectrometer at 400.13 and 100.61 MHz respectively, at 298K. The chemical shifts (δ) are reported in ppm relative to solvent residual signal. The coupling constants (J) are reported in Hertz (Hz). The melting points were measured by B-540 melting point analyzer. High Resolution Electro-spray Ionization Mass Spectra (HR-ESI-MS) were obtained from UBP-Start (Clermont-Ferrand, France). The infrared spectra were recorded on a Nicolet 5700 FTIR spectrometer using the KBr pellet technique in the $4000 - 400\text{ cm}^{-1}$ region.

The photoluminescence spectra were recorded with a Jobin-Yvon set-up consisting of a xenon lamp operating at 400 W and two monochromators (Triax 550 and Triax 180) combined with a cryogenically cold charge coupled device (CCD) camera (Jobin-Yvon Symphony LN2 series) for emission spectra and with a Hamamatsu 980 photomultiplier for excitation ones. One photon excited (OPE) luminescence intensity dependence and decays were obtained by pulsed excitation using a Jobin-Yvon LA-04 Nitrogen Laser (337.1 nm, 5ns pulse, 25Hz) and analyzed through a Jobin-Yvon HR 1000 monochromator, the detector was a R1104 Hamamatsu photomultiplier tube. Fluorescence decays were recorded with a Lecroy 9310A-400 MHz digital oscilloscope. Quantum yields efficiencies were measured using C9920-02G PL-QY measurement system from Hamamatsu. The set-up consisting of a 150W monochromatized Xe lamp, an integrating sphere (Spectralon Coating, $\phi = 3.3$ in.) and a high sensibility CCD camera.

Results and discussion

Rare-earth-free Phosphors

The phosphors have been classified in 3 different groups due to their structure and their emission range upon 365-nm UV light irradiation (Figure 1). These phosphors were selected since they emit the three primary colors under ultraviolet (UV light excitation, which should be compatible with the commercial UV-LEDs at 365 nm.²²⁻²⁴ The synthesis of these phosphors is straightforward and the classical techniques of characterization (^1H and ^{13}C -NMR, IR spectroscopy,

and mass spectrometry) were carried out to identify and confirm their structural properties (see Experimental Section). The luminescence quantum yield of phosphors in solid state compound as well as the emission spectrum were also recorded in order to study their optical characteristics.

The first group of phosphors presents the changes in the alkyl chain length of n-alkylamine part. The emission spectra recorded after excitation at the appropriate wavelength (Table 1) show a wide luminescence from 400 – 600 nm with the maximum in blue-light emission region. The alkyl chain length of n-alkylamine part can also affect the absolute quantum yield.

The second group of luminescent materials which involves 4-dicyanomethylene-2, 6-distyryl-4H-pyran derivatives were studied. Indeed, some kinds of 4-dicyanomethylene-2, 6-distyryl-4H-pyran have been widely studied as the well-known red emitters for lasers and organic light emitting diode devices²⁵⁻²⁸. The development of these kinds of phosphors in solid-state for LEDs applications might be a great challenge. The emission spectra of phosphors recorded after excitation at the appropriate wavelength show a wide luminescence from 500 – 900 nm with the maximum in red-light emission region. It is possible, however, that the conjugated structure in the molecules that induces the bathochromic shift in emission^{29, 30} is not enough and causes a drop in the absolute quantum yield

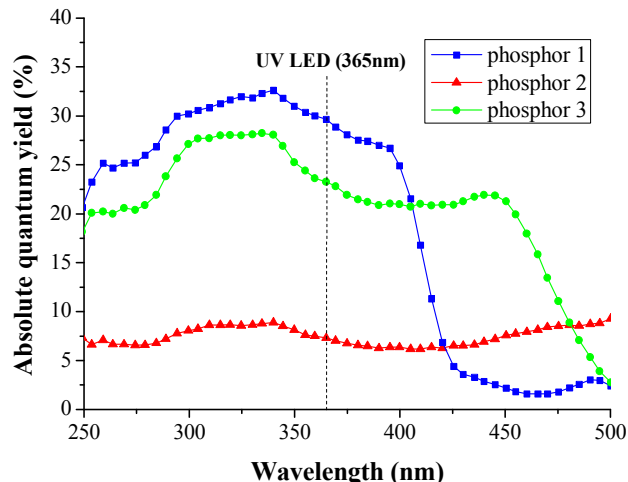
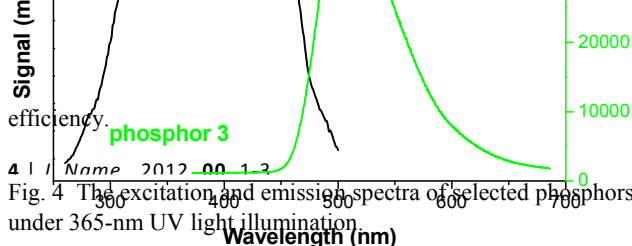
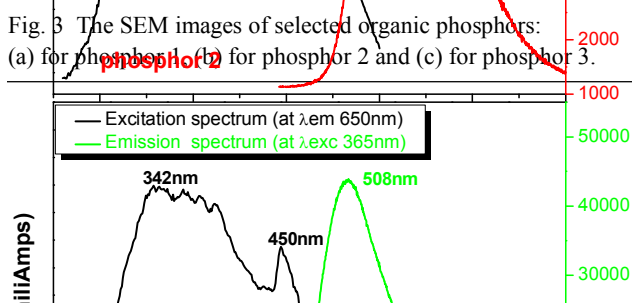
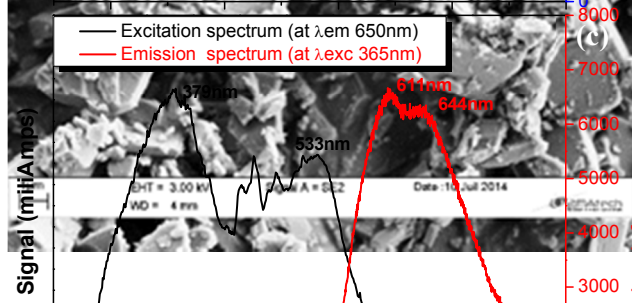
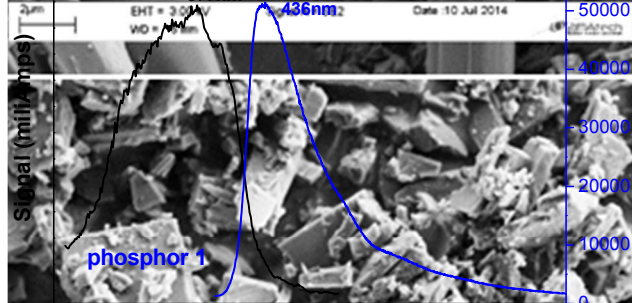
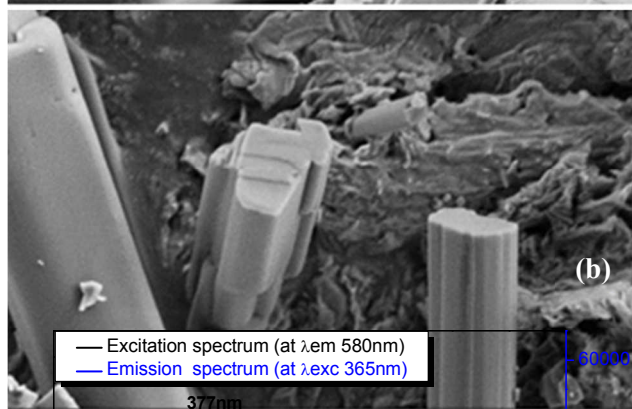
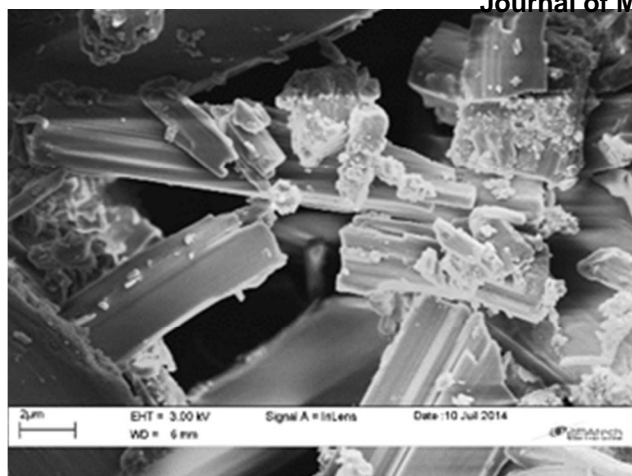


Fig. 2 The absolute quantum yield efficiency of three phosphors presented between 250 - 500 nm light illuminations.



The phosphor in the third group consists of an aluminum complex based on methyl pyrazinyl ketone benzoyl hydrazone ligand. This kind of phosphor is of interest due to its exceptional luminescent properties in solution. Thus, the study of the phosphor in solid-state is of interest and also a challenge for LEDs applications. The absorption and emission spectra of phosphor show the intense green emission under UV excitation with the absolute quantum yield at 28%.

According to all phosphors reported previously, the compounds in each group having the best value in the absolute quantum yield efficiency were chosen. A phosphor with hexylamino part ($n=6$) in the first group and one with phenyl part in the second group have the highest emission intensity and the greatest in absolute quantum yield at 33% and 14%, respectively. The phosphor of 2-(1-hexyl-2,6-dimethylpyridin-4H-ylidene)malononitrile in group 1, 4-dicyano methylene-2,6-distyryl-4H-pyran in group 2, and Al-MPBH complex in group 3 were selected for further study and named as phosphor 1, phosphor 2 and phosphor 3, respectively. These phosphors with the three primary colors could be associated with commercial UV-LEDs at 365 nm after mixing them in the proper proportion to achieve the white emission over a wide range of excitation wavelength (Figure 2).

Fig. 3 The SEM images of selected organic phosphors: (a) for phosphor 1, (b) for phosphor 2 and (c) for phosphor 3.

Fig. 4 The excitation and emission spectra of selected phosphors under 365-nm UV light illumination.

In order to study the typical morphology of the prepared phosphors, SEM measurements were carried out. The SEM images of 2-(1-hexyl-2,6-dimethylpyridin-4H-ylidene)malononitrile (phosphor 1), phosphor 4-dicyanomethylene-2,6-distyryl-4H-pyran (phosphor 2), and Al-MPBH complex (phosphor 3) are shown in Figure 3a, 3b and 3c. It is observed that the microstructure of phosphor1 consists of rod-like agglomerates of rectangular crystals with an average size below 10 μm in width. The SEM image of phosphor 2 displays the clear rod-like structures with 4 μm in diameter. The image of phosphor 3 shows the rectangular-shaped structure and loosely agglomeration, which are varied between 1 – 10 μm in size.

–Table 1 The optical characteristics of organic phosphors studied.

Phosphors	$\lambda_{\text{excitation}}^{\text{max}}$ (nm)	$\lambda_{\text{emission}}^{\text{max}}$ (nm)	QYs (%)
Group 1 (alkyl chain, n)			
Methylamine (n=1)	396	462	7
Butylamine (n=4)	371	451	14
Hexylamine (n=6)	377	436	33
Octylamine (n=8)	389	482	15
Group 2 (aromatic, Ar=)			
Phenyl	379	611	14
Naphthalene	382	624	4
Anthracene	377	681	3
2-pyridine	375	585	7
4-methoxyphenyl	351	618	11
Group 3			
Al ³⁺ - Schiff complex	342	508	28

phosphors, SEM measurements were carried out. The SEM images of 2-(1-hexyl-2,6-dimethylpyridin-4H-ylidene)malononitrile (phosphor 1), phosphor 4-dicyanomethylene-2,6-distyryl-4H-pyran (phosphor 2), and Al-MPBH complex (phosphor 3) are shown in Figure 3a, 3b and 3c. It is observed that the microstructure of phosphor1 consists of rod-like agglomerates of rectangular crystals with an average size below 10 μm in width. The SEM image of phosphor 2 displays the clear rod-like structures with 4 μm in diameter. The image of phosphor 3 shows the rectangular-shaped structure and loosely agglomeration, which are varied between 1 – 10 μm in size.

Figure 4 gathers the emission spectra of the selected phosphors.

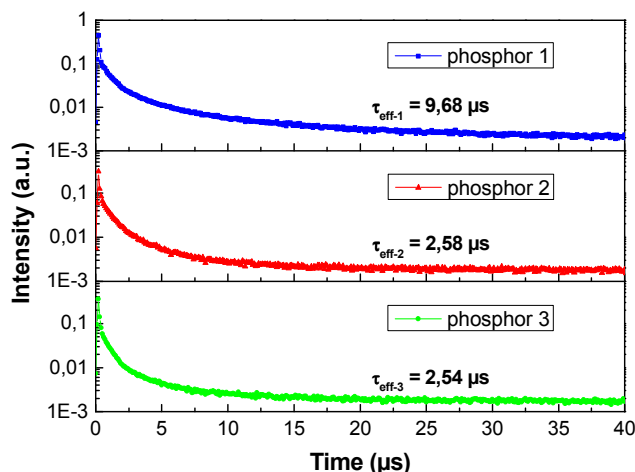


Fig. 5 The luminescence decay curves for the selected phosphors collected upon 337.1 nm excitation at 300K.

The emission spectra of phosphor 1, 2 and 3 exhibit a broad emission in visible range with the maximum wavelength at 446, 695 and 503 nm, respectively. The excitation spectra are broad notably for phosphors 2 and 3. The extent of the excitation spectra can be an indication of the contribution of intramolecular charge transfer (ICT) through the $\pi\pi^*$ excited states. The $\pi\pi^*$ are characterized by small shift since the peak positions of the related excitation bands lie at around 377, 379 and 342 nm for phosphor 1, 2 and 3 respectively. The band peaking at 533 and 450 nm for phosphor 2 and 3 can be attributed to the ICT.

The emission intensity of phosphor 3 was found to be weak compared to others. In order to produce a white light emission, the concentration of each phosphor in the mixed component should be considered. Since the emission spectra of these phosphors show a very broad band in the visible region, the combination of the phosphors might exhibit a high color rendering index (CRI), which is the quantitative measure to display the color of an irradiated object in comparison with a natural light (CRI = 100).³¹ Based on the emission spectra recorded in this experiment, the concentration of phosphors will be adjusted in the silicone support in order to achieve the white emission region.

To study the nature of emitting excited states of the phosphors, the luminescence lifetime of phosphors at room temperature using a pulsed laser excitation at 337.1 nm were measured as shown in Figure 5. In first approach, the luminescence decay time were calculated using the effective emission decay's equation according to R. Pazik³² where $I(t)$ is the luminescence intensity at time t corrected for the background and the integrals are evaluated on a range $0 < t < t_{\text{max}}$ and $t_{\text{max}} \gg \tau_m$. Using the fitted curves, the effective emission decay times were calculated to be approximately 9.68, 2.58 and 2.54 μs for phosphors 1, 2 and 3, respectively. The selected phosphors reported the long luminescence lifetime (in microseconds) can confirm that they are phosphorescent.

$$\tau_m = \frac{\int_0^{\infty} tI(t)dt}{\int_0^{\infty} I(t)dt} \cong \frac{\int_0^{t_{\text{max}}} tI(t)dt}{\int_0^{t_{\text{max}}} I(t)dt} \quad (1)$$

However, as classically used for organic compounds the decays can be also fitted by two exponential functions. The derived time constants from the fits are 0.74 and 5.1 μs for phosphor 1, 0.71 and 3.2 μs for phosphor 2, and 0.43 and 2.33 μs for phosphor 3. Despite a possible emission arising from the ICT, these values are very high and can indicate that the major part of emitting light arises from the triplet state (phosphorescence). The contribution of the long components of the decay times to the global emission are weak since they reach 15%, 15.5% and 13 % for phosphors 1, 2 and 3 respectively. This contribution is assumed to be due to the single molecules not aggregated while the short contribution may come from aggregates into which the distances between the emitting species are short enough to increase efficient energy transfer leading to the decrease of radiative emission. The important contribution of the short component (more than 80 %) can be explained by the synthesis process which can be not enough efficient to prevent agglomeration.

Table 2 The CIE color coordinates, color temperature (CCT), color rendering index (Ra) and luminous efficacy of two composite films under 365-nm UV light illumination.

Film	Composition in silicone polymer film				CIE (x, y)	QE	Ra	CCT (K)
A	Phosphor 1 14.18%	Phosphor 2 0.44%	Commercial YAG: Ce 0.38%	Silicone polymer 85%	(0.366, 0.362)	11.3%	77.3	4315
B	Phosphor 1 14.00%	Phosphor 2 0.72%	Phosphor 3 0.38%	Silicone polymer 85%	(0.378, 0.398)	11.0%	75.4	4214

The thermal properties of selected phosphors were investigated by thermogravimetric analysis (TGA), which was carried out under normal atmosphere at the fixed heating rate of 10°C/min. As shown in figure 6, the first weight loss of phosphors 3 was recorded at 150°C and at 250°C for phosphor 1 and phosphor 2. The results provide the desirable thermal properties of these phosphors for the normal operating conditions of remote-type phosphor reported to be between 40-90°C.³³⁻³⁵

Figure 7 presents the temperature-dependent emission intensity of selected phosphors. However, the emission intensity of phosphors drops significantly with increasing temperature from room temperature to 150°C. Figure 8 shows the time-dependent relative emission intensity of selected phosphors upon continuously excitation at temperature of 110°C. With increasing time, the intensity decrease importantly from 0 to 4 hours. As shown in Fig. 8, the relative emission intensity of selected phosphors becomes less stable at higher temperature in spite of the fact that they present the good thermal properties at that temperature as reported previously. Our results confirm that four luminescent materials have low thermal stability, especially at the operating temperature of LEDs. Ongoing studied on heat protection using silica or silicone precursors are aimed to better enhancing thermal stability of these phosphors.³⁶

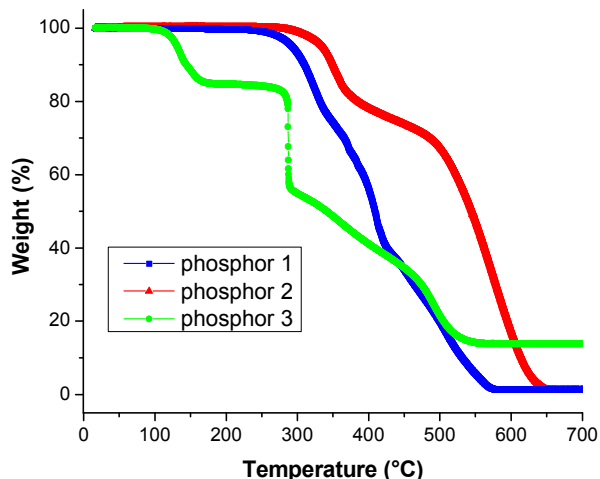


Fig. 6 TGA curves of selected phosphors.

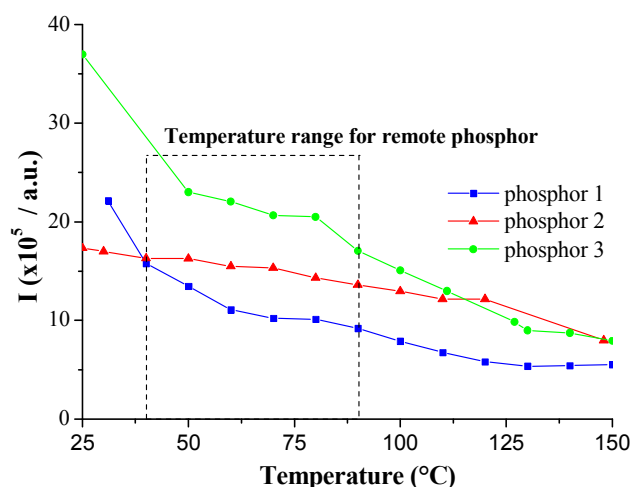


Fig. 7 The temperature-dependent emission intensity of selected phosphors.

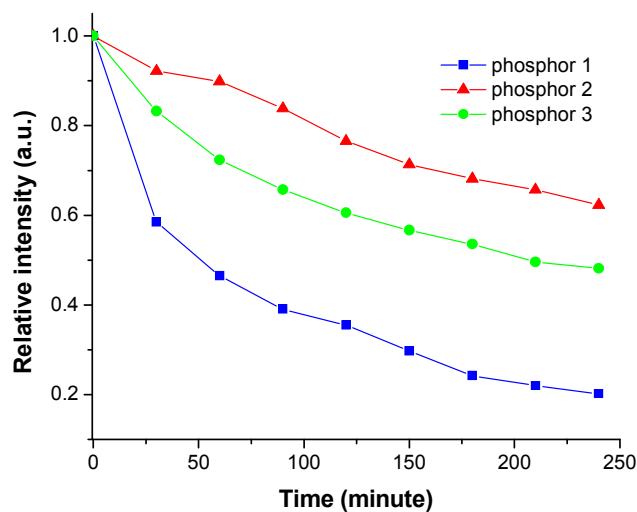


Fig. 8 The time-dependent relative emission intensity of selected phosphors upon excitation continuously at temperature of 110°C.

Composite Films with Silicone

The composite phosphor films obtained after solvent evaporation have a thickness between 190 – 250 μm , and are remarkably flexible, robust, and free standing. It should be noted that, however, the composite films are opaque but slightly translucent due to the thickness and the variation of compositions of phosphors within the films (15%w/w of phosphors in films).

The color point of composite phosphor films is defined according to the convention of the Commission Internationale de l'Éclairage (CIE) in a normalized two-dimensional color coordinate system (Figure 9a). In order to verify the color of composite phosphor films, the films are deposited on the cup holder of UV LEDs chip (365 nm excitation) as a remote phosphor configuration. The CIE color coordinates of various composite phosphor films are reported in Table 2. The concentration of phosphors was controlled and adjusted to achieve the white emission region. In this case, the concentration of phosphor 1, 2, and 3 were fixed at 0.72%, 14% and 0.38% by weight in the film B, respectively. The film A was prepared using phosphor 1 (0.44% w/w), 2 (14.18% w/w) and the commercial YAG: Ce (0.38%w/w) in order to compare its optical properties.

The emission spectra of composite phosphor films recorded after excitation with UV-LEDs at 365 nm show a broad emission wavelength between 400 and 800 nm with two maxima around 460 and 570 nm (Figure 9b). The phosphor 2 was added to the composite phosphor films in order to improve the red components of emission spectra. The color coordinates of film A (0.366, 0.362) and film B (0.378, 0.398) are closed to the theoretical white color as $(x, y) = (0.333, 0.333)$. The absolute quantum efficiencies of films are about 11% under 365-nm UV light illumination. However, our composite films are still requiring the improvement of the luminous efficiency due to the high values reported for a white LEDs using rare-earth activated nitride phosphors³⁷ and for a white LEDs using red quantum dots (CuInS_2) and green phosphors.³⁸ Furthermore, the CRI values is lower than 90, which is the condition for the interior WLEDs lighting requirement.³⁹ These kinds of composite films based on phosphors need more researches to overcome these challenges and further study for straightforward development of better performance in lighting applications.

Conclusions

Rare-earth-free – phosphors based on materials have been synthesized by traditional methods that are quite easy and rapid. The luminescent materials exhibit a broad absorption in UV and blue regions and a strong emission, which can be used to generate white light upon excitation with UV/blue commercial LEDs. When excited by a UV LEDs, the composite films containing a phosphors mixture lead to a white emission with a CRI > 75 and a color temperature close to 4000 K. However, their thermal stability during emission at high temperature it has be improved and becomes a great challenge for phosphors based on luminescent materials. Further work should be dedicated to determining the novel method to protect these phosphors from thermal problems. Therefore, their encapsulation inside an inorganic shell is currently under investigation.

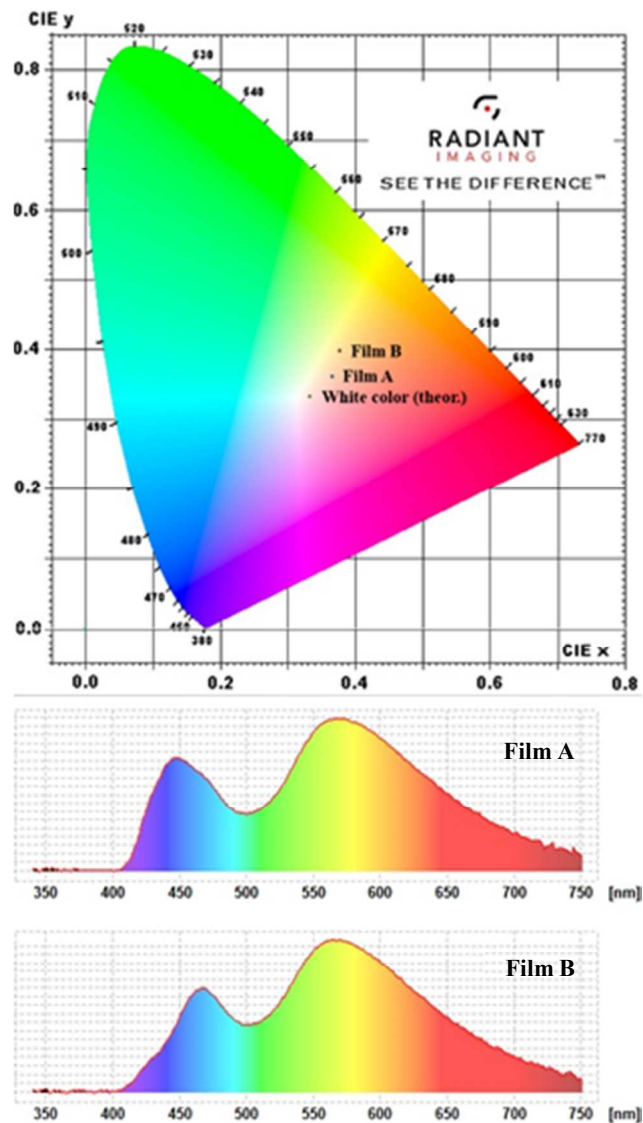


Fig. 9 (a) CIE color coordinates of white LEDs based on the composite mixed phosphor films excited by a UV LED. (b) The emission spectra of films-based white LEDs.

Acknowledgements

The authors thank “Conseil Régional d’Auvergne” and Auvergne region for financial support and Anne-Marie Gélinaud (2Matech, Aubière) for SEM observations.

Notes and references

- S. Shionoya and W. M. Yen, *CRC Press: Boca Raton, FL*, **1998**.
- G. Blasse, *J. Alloys Compd.*, **1995**, **225**, 529-533.
- V. Bachmann, C. Ronda, O. Oeckler, W. Schnick and A. Meijerink, *Chem. Mater.*, **2008**, **21**, 316-325.
- H. S. Jang, H. Yang, S. W. Kim, J. Y. Han, S.-G. Lee and D. Y. Jeon, *Adv. Mater.*, **2008**, **20**, 2696-2702.
- A. A. Setlur, W. J. Heward, M. E. Hannah and U. Happek, *Chem. Mater.*, **2008**, **20**, 6277-6283.
- S. Ye, F. Xiao, Y. X. Pan, Y. Y. Ma and Q. Y. Zhang, *Materials Science and Engineering: R: Reports*, **2010**, **71**, 1-34.
- P. F. Smet, A. B. Parmentier and D. Poelman, *J. Electrochem. Soc.*, **2011**, **158**, R37-R54.
- M. R. Krames, O. B. Shchekin, R. Mueller-Mach, G. Mueller, L. Zhou, G. Harbers and M. G. Craford, *J. Display Technol.*, **2007**, **3**, 160-175.
- W. Sun, M. Shatalov, J. Deng, X. Hu, J. Yang, A. Lunev, Y. Bilenko, M. Shur and R. Gaska, *Appl. Phys. Lett.*, **2010**, **96**, -.
- H. Hirayama, Y. Tsukada, T. Maeda and N. Kamata, *Appl. Phys. Express*, **2010**, **3**, 031002.
- A. Fujioka, T. Misaki, T. Murayama, Y. Narukawa and T. Mukai, *Appl. Phys. Express*, **2010**, **3**, 041001.
- H. Hirayama, S. Fujikawa, N. Noguchi, J. Norimatsu, T. Takano, K. Tsubaki and N. Kamata, *physica status solidi (a)*, **2009**, **206**, 1176-1182.
- Y. Zhu and N. Narendran, *Japanese Journal of Applied Physics*, **2010**, **49**, 100203.
- H. Luo, J. K. Kim, E. F. Schubert, J. Cho, C. Sone and Y. Park, *Appl. Phys. Lett.*, **2005**, **86**, -.
- Y.-H. Won, H. S. Jang, K. W. Cho, Y. S. Song, D. Y. Jeon and H. K. Kwon, *Opt. Lett.*, **2009**, **34**, 1-3.
- M. Humphries, *Congressional Research Service*, **2013**.
- T. Ogi, Y. Kaihatsu, F. Iskandar, W.-N. Wang and K. Okuyama, *Adv. Mater.*, **2008**, **20**, 3235-3238.
- W.-N. Wang, T. Ogi, Y. Kaihatsu, F. Iskandar and K. Okuyama, *J. Mater. Chem.*, **2011**, **21**, 5183-5189.
- Y. Kaihatsu, W.-N. Wang, F. Iskandar, T. Ogi and K. Okuyama, *J. Electrochem. Soc.*, **2010**, **157**, J329-J333.
- T. Ogi, F. Iskandar, A. B. D. Nandiyanto, W.-N. Wang and K. Okuyama, *J. Chem. Eng. Jpn.*, **2012**, **45**, 995-1000.
- M. Meneghini, M. Dal Lago, N. Trivellin, G. Meneghesso and E. Zanoni, *Device and Materials Reliability, IEEE Transactions on*, **2013**, **13**, 316-318.
- Z.-C. Liao, Z.-Y. Yang, Y. Li, B.-D. Wang and Q.-X. Zhou, *Dyes Pigm.*, **2013**, **97**, 124-128.
- L. L. Woods, *J. Am. Chem. Soc.*, **1958**, **80**, 1440-1442.
- M. S. Shin, S. J. Lee, S. M. Chin, S. H. Lee, D. M. Pore, Y. Park, S.-G. Lee and K.-J. Hwang, *Bull. Korean Chem. Soc.*, **2011**, **32**, 3152-3154.
- C. Jianzhong, H.-J. Suh and S.-H. Kim, *Dyes Pigm.*, **2006**, **68**, 75-77.
- D.-H. Hwang, J.-D. Lee, H.-J. Cho, N. S. Cho, S. K. Lee, M.-J. Park, H.-K. Shim and C. Lee, *Synth. Met.*, **2008**, **158**, 802-809.
- H. Tong, Y. Dong, M. Häußler, Y. Hong, J. W. Y. Lam, H. H. Y. Sung, I. D. Williams, H. S. Kwok and B. Z. Tang, *Chem. Phys. Lett.*, **2006**, **428**, 326-330.
- C.-W. Chang, Y.-T. Kao and E. W.-G. Diau, *Chem. Phys. Lett.*, **2003**, **374**, 110-118.
- M. Sauer, J. Hofkens and J. Enderlein, in *Handbook of Fluorescence Spectroscopy and Imaging*, Wiley-VCH Verlag GmbH & Co. KGaA, **2011**, pp. 1-30.
- T. Itoh, *Chemical Reviews*, **2012**, **112**, 4541-4568.
- J. Yu, Y. Yin, W. Liu, W. Zhang, L. Zhang, W. Xie and H. Zhao, *Org. Electron.*, **2014**, **15**, 2817-2821.
- R. Pązik, D. Hreniak, W. Stręk, A. Speghini and M. Bettinelli, *Opt. Mater.*, **2006**, **28**, 1284-1288.
- M. Yazdan Mehr, W. D. van Driel and G. Q. Zhang, *Microelectronics Reliability*, **2014**, **54**, 1544-1548.
- M. Dal Lago, M. Meneghini, N. Trivellin, G. Mura, M. Vanzi, G. Meneghesso and E. Zanoni, *Microelectronics Reliability*, **2012**, **52**, 2164-2167.
- W. Falicoff, **2008**, p. Medium: ED.
- A.-C. Franville, D. Zambon, R. Mahiou and Y. Troin, *Chem. Mater.*, **2000**, **12**, 428-435.
- R.-J. Xie, N. Hirotsaki, Y. Li and T. Takeda, *Materials*, **2010**, **3**, 3777-3793.
- B. Chen, Q. Zhou, J. Li, F. Zhang, R. Liu, H. Zhong and B. Zou, *Opt. Express*, **2013**, **21**, 10105-10110.
- G. He, J. Xu and H. Yan, *AIP Advances*, **2011**, **1**.